COMPREHENSIBLE MODEL OF AMPLITUDE NONLINEARITIES IN PIEZORESISTIVE-FORCE SENSORS

L. Paredes-Madrid and P. Gonzalez de Santos
Centre for Automation and Robotics UPM-CSIC, Ctra. Campo Real Km 0,2, 28500 Arganda del Rey, Madrid, Spain

Keywords: Piezoresistive, force, Sensor, Nonlinear, Model, Tanh, Piezocapacitive, Flexiforce.

Abstract: This article upgrades the RC linear model presented for the piezoresistive-force sensors. Amplitude nonlinearity was found in sensors conductance, and a characteristic equation was formulated for modeling it. By using such equation, it is possible to determine sensor sensitivity for any driving voltage below 1V. This model considerable improves the plug-and-play capability of the sensor. However, sensor conductance is unsatisfactory modeled by such equation when the input voltage goes over 1V. We present an approach for such driving condition.

1 INTRODUCTION

Piezoresistive force sensors have demonstrated to be a good solution for applications demanding non-invasive force readings (Kong et al., 2008; Monroy et al., 2009). However, the relative low repeatability and considerable hysteresis of such sensors, compared to load cells (Vecchi et al., 2000), limit their use to applications where accuracy is not as relevant as the size of the sensor involved (Lebosse et al., 2008).

On the other hand, load cells have demonstrated to be a trustable-force-measurement device in many different systems (Muller et al., 2010) demanding high reliability and accuracy, i.e., force control applications (Sijs et al., 2008) and rehabilitation (Goto et al., 2005). There are several reasons, besides high repeatability, for using load cells: they are available in different sizes and force ranges, they can perform force readings in multiple axes and can withstand overload forces without suffering damages. Dynamic response of load cells is also exceptional, while exhibiting negligible time drift. The main disadvantages of load cells are based in their large bulk and heavy weight, requiring that when a new robot or force control system is under design, load-cell bulk and weight must be taken into account from the early stages of design, since load-cell mass is usually comparable with the system mass where it is used.

In certain research fields as biomechanics, biomedical engineering and haptics, it is necessary to perform non-invasive force readings which are not possible to carry out by using the abovementioned-bulky load cells. Whether if it is necessary to measure contact force on a knee joint (Sawaguchi et al., 2009), or measure grasp force of a human hand (Castro & Cliquet Jr, 2002), within many other applications (Kazerooni et al., 2005; Ahroni et al., 1998), a low profile, light-weight sensor must be used in order to meet the limited space requirements of the task. Piezoresistive force sensors are the best solution since they can be fitted in many applications without requiring substantial changes in the mechanical layout. However, as mentioned previously, they lack of good repeatability and exhibit considerable hysteresis compared to load cells. We are interested in improving piezoresistive-sensors performance with the aim of using them in tele-operation devices specially those devoted to remote handling activities for the maintenance and repair of nuclear fusion installations (Ibarra et al., 2010)

Previous works (Paredes-Madrid, Torruella et al., 2010; Paredes-Madrid, Emmi et al., 2010) have demonstrated that the repeatability of piezoresistive force sensor may be increased by performing capacitance readings under AC sourcing. The method detailed in (Paredes-Madrid, Torruella et al., 2010) consists in reading sensor's conductance and capacitance by applying DC and sine waveforms, thereby; it is possible to perform a multivariable estimation of force which dramatically reduces force estimation errors.

In (Paredes-Madrid, Emmi et al., 2010), a RC-parallel-electrical model was identified for the

Paredes-Madrid L. and Gonzalez de Santos P..
COMPREHENSIBLE MODEL OF AMPLITUDE NONLINEARITIES IN PIEZORESISTIVE-FORCE SENSORS.
DOI: 10.5220/0003453604050410
In *Proceedings of the 8th International Conference on Informatics in Control, Automation and Robotics* (ICINCO-2011), pages 405-410
ISBN: 978-989-8425-74-4

Piezoresistive Force Sensor (PFS) model FlexiForce® A201-100, also, the sensor exhibited a nonlinear response when the frequency of the driving signal went over a determined limit conveniently named as the divergent frequency. However, we have recently found that the sensor exhibits additional nonlinearities related with the amplitude of the driving signal, and thus the RC model and the corresponding equations must be adjusted to embrace the newly-found-amplitude nonlinearity.

This paper reviews the RC model for the A201-100 force sensor which will be referred from now on as PFS. This device was chosen for the study because the manufacturer has developed many specific sensor for research (Culjat et al., 2008), medical (R. A. Lee et al., 2009) industrial and service tasks (Tekscan, 2011), but the results here reported are extendable to other similar devices. Later, amplitude nonlinearity is identified in the sensor and an equation is deducted from experimental data. The feasibility of such equation for modeling sensor conductance is fully tested and demonstrated for driving voltages below 1V. However, it is shown later that the model becomes unsuitable when the sourcing voltage goes over 1V, and so, it is presented an approach for modeling sensor conductance under such driving condition.

2 REVIEW OF THE RC MODEL FOR THE PFS

Previously, the PFS from Fig. 1a was characterized in terms of frequency and transient response to input-sine waves and square waves, respectively. Test results yielded to a RC-parallel-electrical model (see Fig. 1b) for the PFS and consequently a set of equations were presented to model its behavior; however, when the frequency of the driving signal went over a determined value, conveniently named as the divergent point, sensor resistance started to drop as frequency was increased, and the RC model became no longer valid.

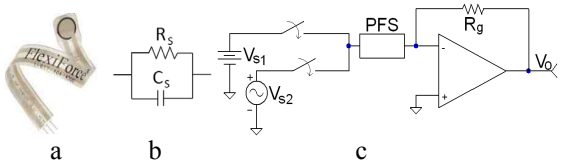

Figure 1: Piezoresistive sensor under study. (a) Picture of the PFS (b) Electrical model of the PFS. (c) Conditioning circuit for measuring forces in the PFS.

This behavior splits sensor response in two differentiated regions: one linear region, when operating below the divergence frequency, where we can model and predict sensor response in terms of phase shift and output amplitude according to the RC theoretical equations, and a nonlinear region, when operating over the divergent frequency, where phase shift and output amplitude become unpredictable.

The typical driving circuit for the PFS is depicted in Fig. 1c. When the sine wave, V_{s2}, is selected as input; the following set of equations taken from (Paredes-Madrid, Torruella et al., 2010) describes sensor response within its linear region of operation.

First, a differential equation can be deduced from the circuit depicted in Fig. 1c with V_{s2} as input:

$$\frac{V_{s2}}{R_s} + C_s \frac{dV_{s2}}{dt} = -\frac{V_o}{R_g} \tag{1}$$

where R_s and C_s are sensor Resistance and Capacitance respectively from the model in Fig.1b, R_g is the feedback resistor in the driving circuit of Fig. 1c with V_o as the output voltage. Given the input:

$$V_{s2} = A_s \sin(2\pi ft) \tag{2}$$

The output voltage, V_o, can be expressed as:

$$V_o = -A_s R_g \left(\frac{\sin(2\pi ft)}{R_s} + 2\pi f C_s \cos(2\pi ft) \right) \tag{3}$$

Second, equation (3) may be rewritten in terms of phase shift, θ, and output amplitude, A_o, as below:

$$V_o = A_o \sin(2\pi ft + \theta) \tag{4}$$

At last, joining (3) and (4) result in:

$$R_s = \frac{R_g A_s}{A_o \cos(\theta)} \tag{5}$$

$$C_s = \frac{A_o \sin(\theta)}{R_g A_s 2\pi f} \tag{6}$$

Equation (6) was previously used in (Paredes-Madrid, Torruella et al., 2010) to measure capacitance changes as force increases. This yielded to demonstrate that the PFS exhibits a piezocapacitive property which is useful for reducing force estimation errors.

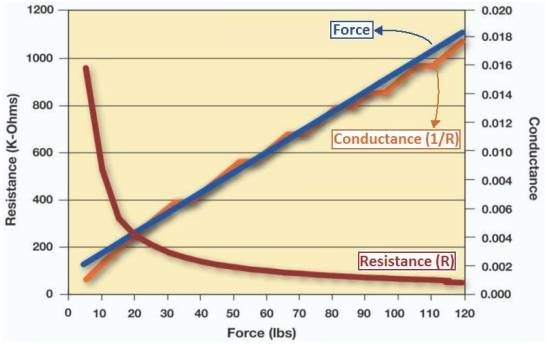

Figure 2: Typical variation of resistance and conductance for an A201-100 FlexiForce® Sensor, image taken from (Tekscan, 2009a). The image legend was modified for better comprehension.

3 AMPLITUDE NONLINEARITY OF THE PFS UNDER DC SOURCING

Besides the already identified frequency nonlinearity, the PFS exhibits amplitude nonlinearity. Initially, we only study such nonlinearity for input voltages within the range (-1V, 1V), and then we present an approach for higher input voltages. The analysis of amplitude nonlinearity must be split in two because the sensor exhibits quasi-different responses depending on the input voltage applied.

3.1 Modelling Amplitude Nonlinearity for Input Voltages below 1V

If we choose the DC source, V_{s1}, as the input of the driving circuit in Fig. 1c we obtain a DC output voltage, V_o, which changes linearly, see Fig. 2 (Tekscan Inc, 2009a) , as the applied force on the sensor increases. This response has been thorough described by sensor manufacturer (Tekscan Inc, 2009b) and in many research articles (Lebosse et al., 2008; Vecchi et al., 2000); this behavior corresponds to the piezoresistive property of the sensor. However, to our knowledge, there is not information available about how the output voltage changes, for a fixed force, when the DC voltage is varied.

In order to study such behavior, we swept the input voltage, V_{s1}, starting at -1V up to 1V and plot de output voltage, V_o, while keeping constant the applied force. In practice, the voltage sweep was made by sourcing the sensor with a low frequency triangle signal of 0.4Hz with peak amplitude of 1V and no offset. The frequency must be kept as low as possible in order to avoid phase-lag effects due to the built-in-sensor capacitance. Forces within the range from 0N to 250N were applied to one PFS device while the output voltage, V_o was recorded.

Figure 3 shows the output voltage for randomly chosen forces of 12N, 45N, 82N and 160N. We have found that the best function that relates the input voltage, V_{s1}, to the corresponding sensor response, V_o, is:

$$V_o = -\frac{1}{q}\operatorname{atanh}\left(\frac{V_{s1}}{k}\right) \quad (7)$$

where k and q are constants. However, it is not convenient to fit k and q in the form presented in (7) because it may yield to complex values in V_o, since the *atanh* domain is restricted to (-1, 1). Thus, it is better, for fitting purposes, to rewrite (7) in terms of the *tanh* function as below:

$$V_{s1} = k\tanh(-q\,V_o) \quad (8)$$

The minus sign in (7) and (8) comes from the negative gain in the inverting amplifier (see Fig. 1c) which is used to drive the sensor. The axes in Fig. 3 are intentionally switched to represent: V_o in the x-axis and V_{s1} in the y-axis with the aim of fitting the data points with (8) instead of with (7). The fitting process is highly confident with a coefficient of determination, R^2, of at least R^2=0.9992 for every applied force and an average value of R^2=0.9995.

Parameters k and q were set to adjust independently for every applied force; however, the independent fitting processes returned values of k almost constant regardless of the exerted force, F,

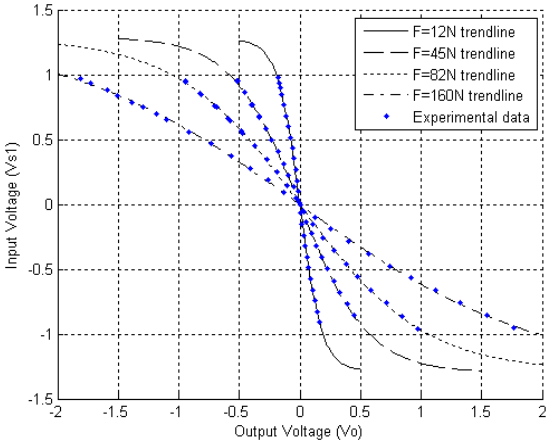

Figure 3: V_{s1} vs. V_o for the PFS for driving voltages below 1V and four different-exerted forces of 12N, 45N, 82N and 160N. The trendline used for each individual fit was a hyperbolic tangent function (8).

whereas q has shown to be hyperbolically dependant on the exerted force; in other words, $1/q$ is a linear function of F. Figure 4 show the variation of k and $1/q$ for different applied forces within the range from 0N to 250N resulting from independent-fitting processes.

Several facts may be taken out from Fig. 3 and Fig. 4 but first, it is necessary to relate (8) with F in order to get a whole view of sensor behavior. For such purpose, we must remember that the sensor exhibits a piezoresistive behavior and thus its conductance, $1/R_s$, may be modeled in terms of the applied force, F, as:

$$1/R_s = mF + b \tag{9}$$

Equation (9) is not explicitly stated in the PFS datasheet (Tekscan Inc, 2009b); however, the sensor manufacturer declares that a linear interpolation between the conductance values and the applied forces can be done. Also, by looking at the conductance curve in Fig. 2, it can be easily deducted that (9) is a valid fit for $1/R_s$. Considering the inverting-amplifier, with feedback resistor R_g, which is used to drive the PFS, it is possible to link (9) with the amplifier characteristic equation:

$$\frac{V_o}{V_{s1}} = -\frac{R_g}{R_s} \tag{10}$$

to obtain:

$$\frac{V_o}{V_{s1}} = -R_g\left(mF + b\right) \tag{11}$$

We must clarify that (11) is not explicitly stated in the PFS datasheet (Tekscan Inc, 2009b). Only (10) is stated in (Tekscan Inc, 2009b), but the manufacturer suggests that sensor sensitivity, m, can be changed by either replacing the feedback resistor, R_g, or by changing the driving voltage, V_{s1}.

According to (11) we may think that changes in V_{s1} produce direct-proportional changes in sensor sensitivity, however experimental results plotted in Fig. 3 yield to different conclusions because the trendline used to fit the experimental data points is not a line.

With the aim of demonstrating that (11) is an approximate expression for fitting the data points from Fig. 3, we take the $1/q$ curve from Fig. 4 and represent it, as linearly dependent on the applied force.

$$1/q = m'F + b' \tag{12}$$

The $1/q$ curve is analogous to the conductance curve of Fig. 2. From now on, we refer to m' and b'

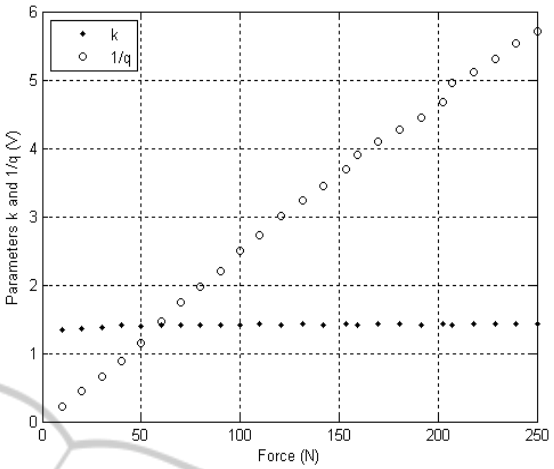

Figure 4: Graph representing the variation of sensor parameters k and q for different exerted forces within the range from 0N to 250N.

as the generalized-sensor parameters, because we demonstrate in the next section that they can predict sensor sensitivity for any input voltage within the range (-1V, 1V). Equation (12) can be substituted into (7) yielding to:

$$V_o = -\left(m'F + b'\right)\operatorname{atanh}\left(\frac{V_{s1}}{k}\right) \tag{13}$$

Nevertheless, we can not state (13) in the same way as (11) because the input voltage, V_{s1}, is part of the *atanh* argument, but if we take only the first term of the *atanh*-taylor series we yield to the following approximate expression:

$$\frac{V_o}{V_{s1}} = \frac{-1}{k}\left(m'F + b'\right) \tag{14}$$

Equation (14) is a non-exact expression of sensor response since it can not model amplitude nonlinearity, likewise (11) is too. The $1/k$ factor, in (14), is analogous to R_g in (11), in the same way that m is analogous to m', b to b' and $1/R_s$ to $1/q$. In fact, (11) is valid if, and only if, the input voltage remains constant during the measurement process; this condition matches for the recommended driving conditions by the manufacturer (Tekscan Inc, 2009b). In case V_{s1} is changed during the measurement process, it is necessary to recalculate the new values of m and b in order to estimate the applied force via (11). But, since neither (11) nor (14) account for the amplitude nonlinearity of the PFS, the new values of m and b would be erroneous. Instead, it is necessary to use the exact expression (13) to correctly estimate the new sensor parameters resulting from the new input voltage.

3.2 Effect of Feedback Resistor in Sensor Response

The effect of feedback resistor R_g in the driving circuit of Fig. 1c and consequently in (13) can be deducted if we notice that R_g only changes the feedback gain of the amplifier without affecting sensor current, thus, changing R_g will produce direct-proportional changes in the output voltage as below:

$$V_o = -\left(\frac{R_g}{R_{ref}}\right)\left(m'F + b'\right)\operatorname{atanh}\left(\frac{V_{s1}}{k}\right) \qquad (15)$$

where R_{ref} is the feedback resistor used during the characterization to obtain the values of *m'*, *b'* and *k*. In case the feedback resistor is changed after the characterization process, the output voltage is multiplied by the ratio R_g/R_{ref} where R_g is the new feedback resistor. Replacing the feedback resistor produces a direct-proportional change in the output voltage because the amplifier is inherently linear, whereas sensor resistance is not. In fact, by linking (7), (10) and (12), we get an expression which shows the non-linear behavior of sensor conductance to changes in the input voltage.

$$\frac{1}{R_s} = \left(m'F + b'\right)\frac{\operatorname{atanh}\left(V_{s1}/k\right)}{V_{s1}R_g} \qquad (16)$$

However, note from (16) that sensor conductance is always linear to force changes as the manufacturer states (Tekscan Inc, 2009b) and the Fig. 2 shows.

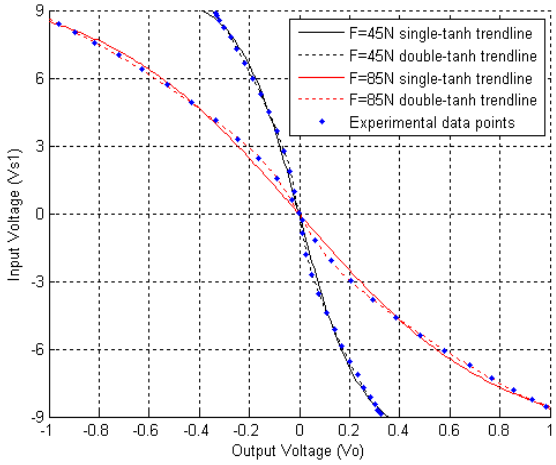

Figure 5: Graph representing the relation of V_{s1} vs. V_o for input amplitudes over 1V and forces of 45N and 85N. Two different trendlines are shown, single (8) and double *tanh* (17).

Equation (15) is the final expression we propose for modeling sensor conductance because it accounts for changes in V_{s1}, as well as to changes in the feedback resistor R_g. By using (15) it is possible to estimate sensor sensitivity under any driving voltages below 1V, or derive an appropriate set of driving conditions (V_{s1} and R_g) to obtain a target sensitivity in the system.

3.3 An Approach to Modeling the Amplitude Nonlinearity for Input Voltages over 1V

In order to study the amplitude nonlinearity for input amplitudes over 1V, it was followed the same procedure described in section 3.1, but now V_{s1} was restricted to a broader range (-9V, 9V). Figure 5 shows the output and input voltages for such condition, but only the responses for two different forces of 45N and 85N are shown for better comprehension.

Initially, the experimental data points were fit in the same way as in section 3.1; this implies using (8) as trendline, but the coefficient of determination did not result as good as before. We propose, as an initial approach, the following curve as a general fit for the data points resulting from V_{s1} over 1V:

$$V_{s1} = k_1 \tanh(-q_1 V_o) + k_2 \tanh(-q_2 V_o) \qquad (17)$$

Trendlines resulting from (8) and (17) are both shown in Fig. 5 for comparison purposes. Note that the data points are pretty close to either trendline, single (8) or double-*tanh* (17), but it is clear that (17) is a better fit specially for the data points which satisfy the condition $|V_{s1}|<3V$. However, in order to use (17) as a valid model, it is necessary a more detailed study with the aim of understanding how the coefficients k_1, k_2, q_1 and q_2 change with every exerted force.

The main problem of proposing (17) as a valid fit for the sensor is based in the large number of coefficients to find and thus the multiple solutions available. We have observed that k_2 remains more or less constant around 1V, whereas k_1 increases with the applied force. But a consistent variation of q_1 and q_2 has not been found yet.

4 CONCLUSIONS

A comprehensive model for the conductance of piezoresistive-force sensors has been developed and tested for input voltages below 1V.

A nonlinear response was identified in sensor conductance corresponding to a hyperbolic tangent function. For voltages over 1V, an approximate model for sensor conductance has been presented but additional tests are required for refining and simplifying it.

ACKNOWLEDGEMENTS

This work has been supported by Madrid Community through the project TECHNOFUSION (S2009/ENE-1679).

REFERENCES

Ahroni, J.H., Boyko, E. J., Forsberg, R., 1998. Reliability of F-scan in-shoe measurements of plantar pressure. *Foot & ankle international/American Orthopaedic Foot and Ankle Society [and] Swiss Foot and Ankle Society*, 19(10), 668.

Castro, M. C., Cliquet Jr, A., 2002. A low-cost instrumented glove for monitoring forces during object manipulation. *Rehabilitation Engineering, IEEE Transactions on*, 5(2), pp. 140–147.

Culjat, M. O., King, C. H., Franco, M. L., Lewis, C. E., Bisley, J. W., et al., 2008. A tactile feedback system for robotic surgery. En *Engineering in Medicine and Biology Society, 2008. EMBS 2008. 30th Annual International Conference of the IEEE*. pp. 1930–1934.

Goto, E., Ohnishi, K., Miyagawa, H., Saito, Y., 2005. Field test of a force control rehabilitation system for quantitative evaluation of the disorder in the upper extremities. En *Rehabilitation Robotics, 2005. ICORR 2005. 9th International Conference on*. pp. 82–85.

Ibarra, A., Perlado, M., Aracil, R., Blanco, D., Ferre, M., et al., 2010. TechnoFusión, a relevant facility for fusion technologies: The remote handling area. *Fusion Engineering and Design*.

Kazerooni, H., Fairbanks, D., Chen, A., Shin, G., 2005. The magic glove. En *Robotics and Automation, 2004. Proceedings. ICRA'04. 2004 IEEE International Conference on*. pp. 757–763.

Kong, Y. K., Lowe, B. D., Lee, S. J., Krieg, E. F., 2008. Evaluation of handle shapes for screwdriving. *Applied Ergonomics*, 39(2), pp. 191–198.

Lebosse, C., Bayle, B., de Mathelin, M., Renaud, P., 2008. Nonlinear modeling of low cost force sensors. En *Robotics and Automation, 2008. ICRA 2008. IEEE International Conference on*. pp. 3437–3442.

Lee, R. A., van Zundert, A. A., Maassen, R. L., Willems, R.J., Beeke, L.P., et al., 2009. Forces applied to the maxillary incisors during video-assisted intubation. *Anesthesia & Analgesia*, 108(1), 187.

Monroy, M., Ferre, M., Barrio, J., Eslava, V., Galiana, I., 2009. Sensorized thimble for haptics applications. In *Mechatronics, 2009. ICM 2009. IEEE International Conference on*. pp. 1–6.

Muller, I., de Brito, R., Pereira, C., Brusamarello, V., 2010. Load cells in force sensing analysis–theory and a novel application. *Instrumentation & Measurement Magazine, IEEE*, 13(1), pp. 15–19.

Paredes-Madrid, L., Emmi, L., de Santos, P., 2010. Improving the performance of piezoresistive force sensors by modeling sensor capacitance. En *Industrial Electronics (ISIE), 2010 IEEE International Symposium on*. Industrial Electronics (ISIE), 2010 IEEE International Symposium on. pp. 458-463.

Paredes-Madrid, L., Torruella, P., Solaeche, P., Galiana, I., Gonzalez de Santos, P., 2010. Accurate modeling of low-cost piezoresistive force sensors for haptic interfaces. In *Robotics and Automation (ICRA), 2010 IEEE International Conference on*. pp. 1828–1833.

Sawaguchi, N., Majima, T., Ishigaki, T., Mori, N., Terashima, T., et al., 2009. Mobile-Bearing Total Knee Arthroplasty Improves Patellar Tracking and Patellofemoral Contact Stress: In Vivo Measurements in the Same Patients. *The Journal of Arthroplasty*.

Sijs, J., Liefhebber, F., Romer, G.W., 2008. Combined Position & Force Control for a robotic manipulator. En *Rehabilitation Robotics, 2007. ICORR 2007. IEEE 10th International Conference on*. pp. 106–111.

Tekscan Inc, 2011. Automotive Door Mounting. Available at: http://www.tekscan.com/automotive-door-mounting-pressure [February 2011].

Tekscan Inc, 2009a. E-book: Force Sensors for Design. Available at: http://www.tekscan.com/flexiforce/force-sensors-for-design [February 2009].

Tekscan Inc, 2009b. FlexiForce®: Single Button FSR. Available at: http://www.tekscan.com/pdf/FlexiForce-Sensors-Manual.pdf [February 2009].

Vecchi, F., Freschi, C., Micera, S., Sabatini, A. M., Dario, P., et al., 2000. Experimental evaluation of two commercial force sensors for applications in biomechanics and motor control. In *5th Ann. Conf. of Int. FES.*